

**Document Version**

Final published version

**Citation (APA)**

Đào, H. T., Hofland, B., Stive, M. J. F., Mai, T., & Ngo, A. (2022). Design Considerations for Brushwood Fences Concerning Bathymetry and Fence Locations. In D. V. Huynh, A. M. Tang, D. H. Doan, & P. Watson (Eds.), *Proceedings of the 2nd Vietnam Symposium on Advances in Offshore Engineering - Sustainable Energy and Marine Planning: Sustainable Energy and Marine Planning* (pp. 238-245). (Lecture Notes in Civil Engineering; Vol. 208). Springer. [https://doi.org/10.1007/978-981-16-7735-9\\_25](https://doi.org/10.1007/978-981-16-7735-9_25)

**Important note**

To cite this publication, please use the final published version (if applicable).  
Please check the document version above.

**Copyright**

In case the licence states “Dutch Copyright Act (Article 25fa)”, this publication was made available Green Open Access via the TU Delft Institutional Repository pursuant to Dutch Copyright Act (Article 25fa, the Taverne amendment). This provision does not affect copyright ownership.  
Unless copyright is transferred by contract or statute, it remains with the copyright holder.

**Sharing and reuse**

Other than for strictly personal use, it is not permitted to download, forward or distribute the text or part of it, without the consent of the author(s) and/or copyright holder(s), unless the work is under an open content license such as Creative Commons.

**Takedown policy**

Please contact us and provide details if you believe this document breaches copyrights.  
We will remove access to the work immediately and investigate your claim.

***Green Open Access added to TU Delft Institutional Repository***

***'You share, we take care!' - Taverne project***

**<https://www.openaccess.nl/en/you-share-we-take-care>**

Otherwise as indicated in the copyright section: the publisher is the copyright holder of this work and the author uses the Dutch legislation to make this work public.



# Design Considerations for Brushwood Fences Concerning Bathymetry and Fence Locations

Hoang Tung Dao<sup>1,2(✉)</sup>, Bas Hofland<sup>2</sup>, Marcel J. F. Stive<sup>2</sup>, Tri Mai<sup>3</sup>, and Anh Ngo<sup>4</sup>

<sup>1</sup> Faculty of Marine Science and Island, Hanoi University of Natural Resources and Environments, 41A Phu Dien, Bac Tu Liem, Hanoi, Vietnam  
dhtung@hunre.edu.vn

<sup>2</sup> Faculty of Civil Engineering and Geosciences, Delft University of Technology, Stevinweg 1, 2628 CN Delft, The Netherlands  
{b.hofland,m.j.f.stive}@tudelft.nl

<sup>3</sup> Faculty of Coastal and Offshore Engineering, Hanoi University of Civil Engineering, 55 Giai Phong, Hai Ba Trung, Hanoi, Vietnam  
trimc@nuce.edu.vn

<sup>4</sup> Faculty of Civil Engineering, Thuyloi University, 175 Tay Son, Dong Da, Hanoi, Vietnam  
anhntt@tlu.edu.vn

**Abstract.** Wooden fences are nature-based supporting structures to restore mangroves in the Mekong Delta. The hydraulic functioning of wooden fences was studied in previous studies. However, the role of bathymetry in the dissipation and damping of waves by wooden fences has not been studied yet. Thus, in this study, a numerical approach is used to find the effect of the position of fences and the foreshore bathymetry, including two particular slopes of 1/200 and 1/500, on wave damping due to wooden fences. The results show that the bottom slope significantly influences the dissipation of incoming waves, the so-called pre-dissipation, before damping by the wooden fences. Differences in pre-dissipation occur between fence locations along the cross-shore slopes. The higher pre-dissipation takes place for wooden fences closer to the land, as the depth-limited wave height at the fence reduces. The efficiency in wave damping of wooden fences is also increasing as the freeboard is becoming larger for the fence located closer landward.

**Keywords:** Wooden fences · Numerical model · SWASH · Bottom slope · Fence locations

## 1 Introduction

In the Mekong Delta, wooden fences are used as a supportive structure for hard structures to reduce the incoming wave energy and to increase the sedimentation rate inside the downstream basin. In the field, wooden fences contain two to three rows of vertical bamboo poles forming a frame to store horizontal brushwood, such as bamboo branches [1–3]. Previous studies reported that a 50% to 80% reduction of the incoming wave heights was found at field measurements [1–3] and from numerical studies [4]. Due to a lack of understanding of flow over wooden fences, Dao et al. (2020) [5] carried out

experiments to indicate the friction coefficients of wooden fences, i.e., the bulk drag coefficient and the Forchheimer coefficients. The bulk coefficient is the most crucial parameter that is applied in the numerical model.

The Mekong deltaic coast is characterized by a very gentle bathymetry with an average slope from 1/500 to 1/1500 [6, 7], creating a very healthy intertidal area for mangroves to develop up to 1500 m without the presence of sea dikes and/or no human interventions [8]. In reality, the mangrove width reduces by up to about 100 m, due to a rate of erosion of 10 to 50 [6]. The erosion also leads to a steeper slope; for example, the slope in Ganh Hao, Bac Lieu is about 1/200 [8]. In other locations, such as Nha Mat, Bac Lieu, the slope is about 1/500 [9]. Research on observing the presence of wooden fences in front of the remaining mangroves and the role of wooden fences in damping incoming waves on different slopes before reaching the mangroves has not yet been found in any publication.

In this study, the wave damping caused by wooden fences on different slopes and different locations is studied. The outline of this study is as follows. Section 1 is the introduction. The methodology and results are in Sects. 2 and 3, respectively. Finally, Sect. 4 is the conclusions.

## 2 Methodology

### 2.1 Bathymetry and Wave Conditions

The intertidal zone of the Mekong Delta is dominated by a tidal range of about 4.0 m with the MSL = 1.95 m, and MHL = 3.95 m [10, 11]. With the gentle slope varying from 1/200 to 1/1500, the intertidal width can be increased up to 1500 m, which provides an area where healthy mangroves are able to grow. In this study, two bottom slopes are used to represent the Mekong deltaic coast. The slopes of 1/200 and 1/500 are found at Nha Mat, Bac Lieu [9], and at Ganh Hao, Bac Lieu [8], respectively.

Wave characteristics are obtained from the study of Tas (2016), based on the wind data at Con Dao station [12] and wave-data from the NOAA wave model (National Oceanic and Atmospheric Administration, 2014). In Table 1, wave conditions at a water depth of 65 m (deep water) with a return period varying from 10 to 50 years are presented. The wave height and wind set-up are obtained from their marginal distributions, but the high correlation that can be expected provides a reasonable and (slightly) safe assumption. From an engineering perspective, the higher return period for a wave condition is normally chosen for a highly safe scenario, directly related to the strength and lifetime of the soft structure. In this study, the wave condition with a return period of 10 years, as given in Table 1, is chosen as wave boundary for the numerical model. The water level is taken as MHL and with a 10-year wind set-up, which amounts to assumed to be five years of this field structure. When designing for a wave condition with a 10-year return period, the probability that this situation will occur during the lifetime is 41%. Hence, this is a condition with a high probability of occurrence, such that the fence should be able to withstand this situation.

**Table 1.** Extreme wave conditions at a water depth of 65 m obtained at Con Dao and Bach Ho station [7].

Return period (y)	Wave period $T_p$ (s)	Wave height $H_s$ (m)	Wind speed $U_{10}$ (m/s)	Wind set-up (m)
<b>10</b>	<b>9.4</b>	<b>5.1</b>	<b>19.7</b>	<b>0.6</b>
20	9.7	5.7	21.9	0.7
25	10.0	5.9	22.6	0.8
40	10.1	6.3	24.1	0.9
50	10.4	6.5	24.8	0.9

## 2.2 Model Description

The numerical models, SWAN and SWASH, are applied to simulate wave propagation and wave interaction with wooden fences on the Mekong deltaic coast. SWAN is a third-generation wave model and is applied for simulating wave parameters in coastal regions. This model is developed by Delft University of Technology based on the action balance equation [13, 14]. On the other hand, SWASH is a time-domain model applied for simulating non-hydrostatic and free-surface, based on non-linear shallow water equations [15].

Due to the lack of offshore bathymetry in the Mekong Delta, the numerical model profile is assumed to be useful from a distance from the coast about 100 km to a water depth of 50 m. In SWASH, the time-consuming computational requirements for such a long distance are very high, leading to an inconvenient computation of the entire domain. Thus, the combination of SWAN and SWASH is needed to calculate wave propagation from the offshore. Additionally, both the SWAN and SWASH models are validated and efficient to produce wave propagation from the offshore to the nearshore region [15].

The domain of both the SWAN and SWASH models is studied in one-dimensional mode (1D) for which one cross-section perpendicular to the coastline is defined in Fig. 1. The length of the computational domain depends on the bottom slope. In the SWAN model, the computation domain is from  $z = -45.0$  m to  $z = +6.0$  m (Fig. 1, bottom panel) with a total of 108 km long. In Fig. 1, the cross-shore profile in the SWAN model is separated into several bottom slopes with a cell grid of 10.0 m. A standard JONSWAP (JOint North Sea Wave Observation Project) shape spectrum with a wave height and peak period with a return period of 10 years is imposed at the left side of the profile at  $z = -45.0$  m.

The computational domain of the SWASH model is much smaller, but has a much higher resolution than the SWAN model. The domain of SWASH is located from a bottom level, MSL-2 m ( $x = -2.4$  km) to  $z = +5.0$  m ( $x = +3.0$  km) with the grid size of 0.25 m. From MSL ( $x = 0.0$  km), the bottom slope of 1:500, as the base slope, is presented in Fig. 2. All scenarios are tested with a sea dike. The wave boundary is imposed at the offshore boundary, using the spectrum output from the SWAN model at  $x = -2.4$  km (see Fig. 1, bottom panel) at a water depth of 3.95 m under the MHL. The wave characteristics are calculated from variance densities, including  $H_s = 1.45$  m,  $T_p$

= 9.4 s, and  $d = 3.95$  m. For all simulations, one vertical layer is applied, the vertical turbulent mixing of viscosity is set as  $3.10^{-4}$ , and the bottom friction as Manning’s roughness is kept the same as in the SWAN model, as 0.038. The further application and boundary conditions are described in [15].

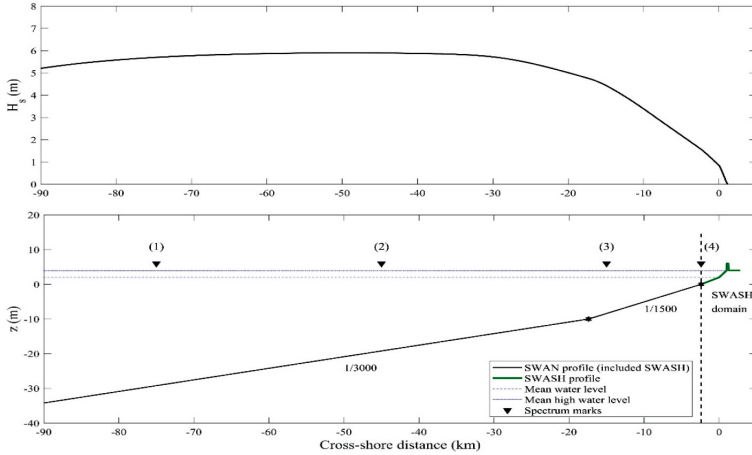


**Fig. 1.** Wave transformation (top panel) and the computational domain in the SWAN model (bottom panel). The SWASH profile (green line) is defined on the right side of the dash line in the bottom panel.

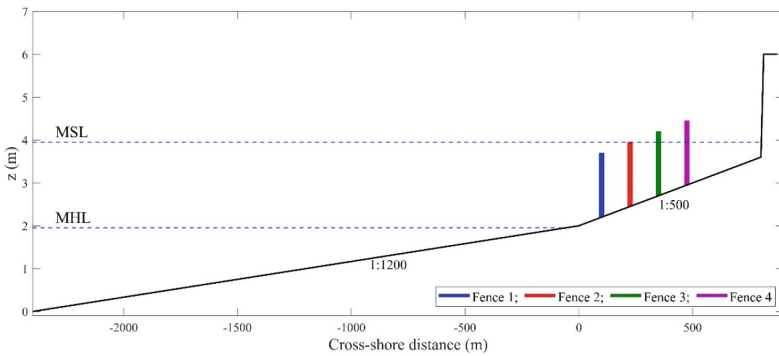


**Fig. 2.** Computational domain of SWASH in the base slope of 1/500. Wooden fences are located at  $x_f$  from 100 m to 500 m.

The vegetation model in SWASH (version 6.01) is applied to simulate wooden fences. The SWASH model was well-validated for the wave-fence interaction aspects [16]. In this model, wave reduction due to an array of stiff cylinders, including horizontal and vertical cylinders, is implemented [17]. For the fence, the brushwood is modelled by horizontal cylinders. The characteristics of a wooden fence are based on Dao et al. (2020) [5], with a branch density of  $N = 603$  cylinders/m<sup>2</sup>, a mean branch diameter of

$D = 0.02$  m, and a bulk drag coefficient of  $\overline{C_D} = 2.0$ . One fence height of 1.5 m is used for all simulations. One thickness, as  $B = 1.2$  m, is tested at each location. In Fig. 2, several cross-shore locations of the wooden fence from the coastline (at MSL),  $x_f$ , are considered from  $x_f = 100$  m to  $x_f = 475$  m corresponding to water depth at the fence toe ( $d$ ) that decrease from 1.75 m to 1.00 m. Moreover, the slope of 1:200 is chosen to compare the wave damping with the base slopes. The wooden fences are set at the same water depth as the base slopes. As a result, the fence locations are changed due to shorter profile of slope 1:200. The design cases for wooden fences of both slopes are presented in Table 2. The water depth at each location is remained constant resulting the constant freeboard ( $R_c$ ) for two slopes.

**Table 2.** Design scenarios for wave damping due to wooden fences.

Cases	$x_f$ (m)		Water depth $d$ (m)	Freeboard $R_c$ (m)	Bottom level $z$ (m)
	Slope 1:500	Slope 1:200			
1	100	40	1.75	-0.25	2.20
2	225	90	1.50	+0.00	2.45
3	350	140	1.25	+0.25	2.70
4	475	190	1.00	+0.50	2.95

### 3 Results

The development of the significant wave height on the cross-shore profile in relation to wooden fences at all locations on the 1:200 and 1:500 slopes is presented in Fig. 3. Generally, the incoming wave is more dissipated on the 1:200 slope (Fig. 3b) than on the 1:500 slope (Fig. 3a). In Fig. 3a, the wave height ( $H_s$ ) at  $x = 95$  m for the first fence position is reduced from 1.03 m to 0.91 m, to 0.78 m, and to 0.66 m on the 1:500 slope for every 125 m. The highest reduction is found at the fence that is located further landwards, mainly due to the effect of depth-induced breaking. For the steeper slopes (1:200) in Fig. 3b,  $H_s$  is dissipated by about 0.12 m for every 50 m, corresponding to locations of wooden fences. It is noted that the dissipation of  $H_s$  on the steeper slope is also faster than on the gentler slope. For example,  $x_f$  at  $x = 95$  m reduces to 0.90 m after 135 m for the 1:200 slope (Fig. 3b), while it needs about 300 m to have a similar value for  $H_s$  for the 1:500 slope (Fig. 3a). Due to the fast dissipation of incoming waves, the wave damping at all locations is also different for both slopes. The higher dissipation before contacting the fence, the so-call pre-dissipation, leads to lower transmission waves for all slopes. For the 1:500 slope in Fig. 3a, the transmitted wave heights ( $H_t$ ) are 0.44 m ( $x = 110$ , blue line), 0.38 m ( $x = 265$  m, red line), 0.31 m ( $x = 360$  m, green line) and 0.26 m ( $x = 485$  m, purple line). The  $H_t$  for the 1:200 slope are slightly higher corresponding to four locations (Fig. 3b). Interestingly, the bottom slope significantly impacts the pre-dissipation rather than the transmitted wave heights. It is due to  $H_t$  being much smaller

than the water depth leading to the lower dispersion rate of transmission waves. The results indicate that the closer to wooden fences, the higher the pre-dissipation of waves.

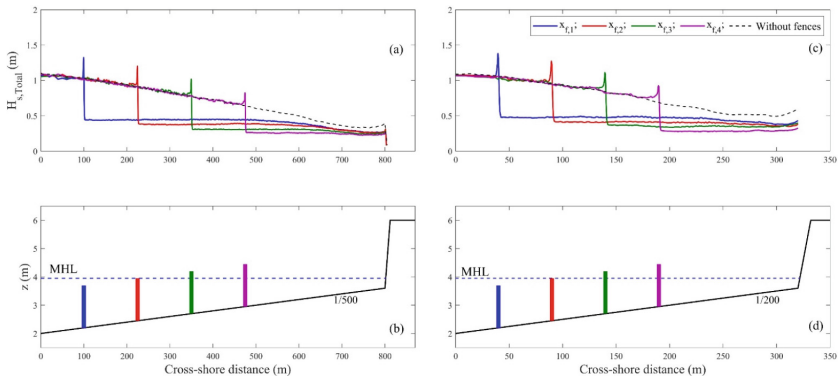


**Fig. 3.** Wave evolution over wooden fences on the 1:200 and 1:500 slopes at all locations. Wave dissipation without fences (dashed line) is indicated as a reference. Wooden fences at three locations are indicated as the same color as wave heights in the bottom panel.

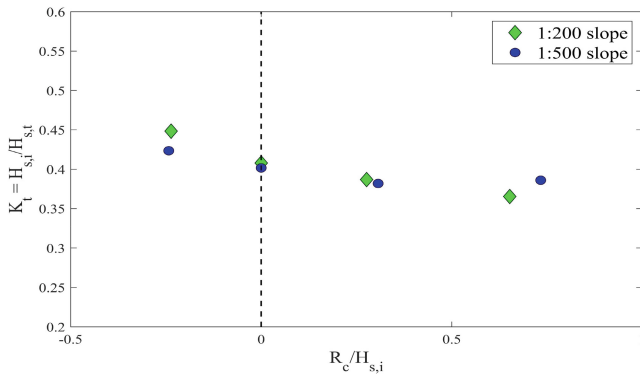


**Fig. 4.** The relationship between the transmission coefficient ( $K_t$ ) and relative freeboard ( $R_c$ ) at two bottom slopes.

As wooden fences move toward the landward side, the fences have a larger freeboard,  $R_c$ , due to the bottom slopes (Fig. 2). The increase of freeboard leads to an increase in the wave damping because less wave overtopping occurs. In Fig. 4, the relationship between the transmission coefficient ( $K_t$ ) and the relative freeboard ( $R_c$ ) is presented for every fence location and all slopes. As can be seen, the  $K_t$  value decreases with the increase of  $R_c$  for all slopes which reaches the lowest value, 0.37 (1:200 slope, green diamond) and 0.39 (1:500 slope, blue circle), at  $R_c$  of 0.65 and 0.73, respectively. In detail, about 60% wave height can be damped by wooden fences at two last locations,  $x_f = 140$  m and 190 m for the steeper slope (Fig. 3c), and  $x_f = 350$  m and 475 m for the gentler slope (Fig. 3d). Figure 4 also points out that the transmission wave on the steeper slope

(green diamond) is higher when fences are submerged, but it is similar to the gentler slope (blue circle) under emerged conditions. The results suggest that for the fence of a constant height, in this case, the steeper a slope, the larger the wave damping. This adds to the fact that wave height, at the seaward side of the fences that are placed more landward, is already lower due to the larger depth-induced wave damping.

## 4 Conclusions

In this study, the numerical model, SWASH, was applied to evaluate the effect of bottom slope on pre-dissipation of waves and damping waves due to wooden fences. The results showed the influence of the bottom slope in pre-dissipation when the higher pre-dissipation occurred at the fence closer to the land. As a fence moves to the landward side, the freeboard is becoming larger, resulting in higher wave damping due to wooden fences.

**Acknowledgements.** The authors gratefully acknowledge the support of the National University of Civil Engineering, Vietnam within the funded project 36-2019/KHXD-TĐ, Delft University of Technology and Hanoi University of Natural Resources and Environments in Vietnam support this research.

## References

1. Van Cuong, C., Brown, S., To, H.H., Hockings, M.: Using Melaleuca fences as soft coastal engineering for mangrove restoration in Kien Giang, Vietnam. *Ecol. Eng.* **81**, 256–265 (2015)
2. Albers, T., San, D.C., Schmitt, K.: Shoreline management guidelines: coastal protection in the lower Mekong delta, vol. 1, pp. 1–124 (2013)
3. Schmitt, K., Albers, T., Pham, T.T., Dinh, S.C.: Site-specific and integrated adaptation to climate change in the coastal mangrove zone of Soc Trang Province, Viet Nam. *J. Coast. Conserv.* **17**(3), 545–558 (2013). <https://doi.org/10.1007/s11852-013-0253-4>
4. Dao, T., Stive, M.J.F., Hofland, B., Mai, T.: Wave damping due to wooden fences along mangrove coasts. *J. Coast. Res.* **34**(6), 1317–1327 (2018). <https://doi.org/10.2112/JCOASTRES-D-18-00015.1>
5. Dao, H.T., Hofland, B., Stive, M.J.F., Mai, T.: Experimental assessment of the flow resistance of coastal wooden fences. *Water* **12**(7) (2020). <https://doi.org/10.3390/w12071910>
6. Phan, L.K., van Thiel de Vries, J.S.M., Stive, M.J.F.: Coastal mangrove squeeze in the Mekong delta. *J. Coast. Res.* 233–243 (2014). <https://doi.org/10.2112/JCOASTRES-D-14-00049.1>
7. Tas, S.: Coastal protection in the Mekong Delta: wave load and overtopping of sea dikes as function of their location in the cross-section, for different foreshore geometries. Delft University of Technology (2016)
8. Phan, L.K.: Wave attenuation in coastal mangroves: mangrove squeeze in the Mekong delta. Delft University of Technology (2019)
9. Thieu Quang, T., Mai Trong, L.: Monsoon wave transmission at bamboo fences protecting mangroves in the lower mekong delta. *Appl. Ocean Res.* **101**, 102259 (2020). <https://doi.org/10.1016/j.apor.2020.102259>
10. Gagliano, S.M., McIntire, W.G.: Reports on the Mekong river delta. Louisiana State Univ Baton Rouge Coastal Studies Inst (1968)

11. Wolanski, E., Huan, N.N., Nhan, N.H., Thuy, N.N.: Fine-sediment dynamics in the Mekong River estuary, Vietnam. *Estuar. Coast. Shelf Sci.* **43**(5), 565–582 (1996)
12. Tran, V.L., Nguyen, D.B., Nguyen, V.T.: On the wind pressure zone map of the Vietnam territory. In: Workshop on Regional Harmonization of Wind Loading and Wind Environmental Specifications in Asia-Pacific Economies (APEC-WW), pp. 1–7 (2004)
13. Booij, N., Holthuijsen, L.H., Ris, R.C.: The “SWAN” wave model for shallow water. In: *Coastal Engineering 1996*, pp. 668–676 (1997)
14. Booij, N., Ris, R.C., Holthuijsen, L.H.: A third-generation wave model for coastal regions: 1. model description and validation. *J. Geophys. Res. Ocean.* **104**(C4), 7649–7666 (1999)
15. Zijlema, M., Stelling, G., Smit, P.: SWASH: An operational public domain code for simulating wave fields and rapidly varied flows in coastal waters. *Coast. Eng.* **58**(10), 992–1012 (2011)
16. Dao, H.T., Hofland, B., Suzuki, T., Stive, M.J.F., Mai, T., Tuan, L.X.: Numerical and small scale physical modelling of wave transmission by wooden fences. *J. Coast. Hydraul. Struct.* **1**(4), 1–21 (2021). <https://doi.org/10.48438/jchs.2021.0004>
17. Suzuki, T., Hu, Z., Kumada, K., Phan, L.K., Zijlema, M.: Non-hydrostatic modeling of drag, inertia and porous effects in wave propagation over dense vegetation fields. *Coast. Eng.* **149**, 49–64 (2019)